Coincidental TID Production by Tropospheric Weather during the August 2017 Total Solar Eclipse

Sebastijan Mrak[1], Joshua Semeter[1], Yukitoshi Nishimura[1], Michael Hirsch[1], and Nithin Sivadas[1]

[1]Department of Electrical and Computer Engineering and Center for Space Physics, Boston University, Boston, MA, USA

Key Points:

- The TIDs previously ascribed to the 2017 total solar eclipse are most likely not associated with the eclipse; they were present at other times.
- The TID pattern, speed, period and wavelength are inconsistent with the bow wave hypothesis. Evidence is presented suggesting a thunderstorm origin.
- The TIDs with mean $\lambda_H \approx 350$ km and $v_H \approx 220$ m/s propagated radially away from the tropospheric storm in east/south-east direction.

Corresponding author: Sebastijan Mrak, Boston University, 8 St. Mary's St., Boston, MA-02215, smrak@bu.edu

Abstract

It has been proposed [*Chimonas and Hines*, 1970], that a total solar eclipse should generate internal Gravity Waves (GWs) that manifest as Traveling Ionospheric Disturbances (TIDs) at ionospheric heights. *Zhang et al.* [2017] recently reported observations of electron density perturbations trailing the region of maximum obscuration, claiming the results as the first unambiguous evidences for eclipse induced bow waves. We present evidence showing extensive TID activity on two consecutive days, the day of the eclipse and the day before. A particularly intense TID concentric wave field emerged from the background ionosphere five hours before the arrival of the totality, and persisted there throughout the eclipse. The apparent center was located over Iowa/South Dakota region, 300 – 500 km north from the eclipse path. We examine concurrent observations of tropospheric and ionospheric weather, and find a great spatiotemporal correlation. TID wave parameters do agree with previous observations and models of thunderstorm generated GWs/TIDs, conversely the wave parameters are an order of magnitude off from modeling results for eclipse generated GWs/TIDs.

1 Introduction

A total solar eclipse is an episodic natural laboratory experiment that provides an incredible opportunity to study the response of the thermosphere, ionosphere, and atmosphere (geospace) to a controlled perturbation. The controlled nature of the experiment is invaluable for testing and validation of physical models. It is therefore crucial to fully understand the observations, including the influence of multiple source mechanisms that may be acting on the system [e.g. *Coster et al.*, 2017; *Mrak* et al., 2018]. Of particular interest in the ionospheric community has been a proposed initiation of atmospheric bow waves [*Chimonas and Hines*, 1970]. The rise of GPS receiver networks has allowed us to map ionospheric features in space and time. The abundance of GPS receivers in the North America and the ability to receive multiple lines-of-sight simultaneously, defines an opportunistic ionospheric imaging tool with unprecedented resolution. A differential TEC (∆TEC) approach has been successfully employed to detect tiny spatially coherent disturbances caused by numerous physical mechanisms [e.g., *Tsugawa et al.*, 2007, 2011; *Nishioka et al.*, 2013; *Grawe and Makela*, 2015; *Azeem et al.*, 2015; *Chou et al.*, 2017].

Hitherto, there are two known reports of possible bow waves imprinted in the ionosphere [i.e., *Liu* et al., 2011; *Zhang et al.*, 2017]. However, both reports rest on weak or questionable foundations. While the former [*Liu* et al., 2011] suffers from sparse spatial sampling (averaging 500 km in longitude), the latter [*Zhang et al.*, 2017] neglected the background space weather during and prior to the eclipse. In this letter, we carefully analyze ionospheric electron density perturbations, ∆TEC, observed before and during the 2017 total solar eclipse, and find no evidence connecting their generation to the eclipse.

Observations of day-side ionospheric activity for two consecutive days revealed a zoo of ionospheric perturbations, among which the most prominent were concentric TIDs propagating from central United States (US) towards east/south-east. The spatiotemporal evolution and wave parameters of these TIDs closely match the "bow waves" reported by *Zhang et al.* [2017]. Using an extended set of ionospheric observations in conjunction with radar maps of weather reflectivity, we show that the TID source is likely to be internal gravity waves (GWs) initiated by a region of persistent thunderstorm activity (convective plumes). The TIDs were, in fact, present in the background ionosphere before the arrival of the eclipse. Additionally, there was very similar TID activity over the same region in space and time on the day before. The source of the TIDs is linked to a tropospheric weather system by virtue of space-time-frequency wave analysis and simultaneous observations of ionospheric and tropospheric weather. Based upon the data analysis we argue that the TIDs on the day of the eclipse were initiated by tropospheric weather rather than the eclipse. We also elaborate on the observational and physical difficulties in linking the observed TIDs to an eclipse source.

2 Methodology

We use CORS and CDDIS publicly available databases with Global Navigation Satellite Systems (GNSS) data which totally account for ~1800 receivers in the continental US. We utilized a standard approach to compute the phase-corrected slant TEC estimates [*Coster et al.*, 1992], converted to vertical (vTEC) via mapping function [*Klobuchar*, 1987] applied at 300 km altitude. We than subtract the background vTEC to obtain differential TEC (ΔTEC) residuals, utilizing variable orders of polynomials [*Mrak* et al., 2018]. The carrier phase based differential approach provides accuracy better to 0.03 TECu [*Coster et al.*, 2012] (1 TECu = $10^{16}e^{-}$/m2). The ΔTEC residuals are then mapped to a geographical map at an altitude of 300 km and then transformed from the naturally irregular spatial grid into a regular grid [e.g., *Azeem et al.*, 2015; *Nykiel et al.*, 2017; *Mrak* et al., 2018] with a resolution of 0.2° × 0.2° (geographical coordinates). The differential approach and excellent spatial coverage (~15,000 spatial points at a given time) allow one to extract coherent spatial features of tiny amplitudes. The spatial extent and appearance of the coherent perturbations are then presented in form of 2D projections. The wave parameters are then extracted using keogram and spectrogram analysis.

3 Observations

Figure 1 shows TEC perturbations on the day of the total solar eclipse (21 August 2017). Starting at 13 UT, a coherent TID wave field emerged over central and eastern US with longitudinal extent ranging from Iowa to the Atlantic, and latitudinal extent from the Gulf of Mexico to Canada. The TIDs were nearly concentric, with an apparent center over the Iowa/South Dakota region. The TIDs were the dominant coherent day-side ionospheric perturbation until the arrival of the eclipse (penumbra) at ~17 UT. During the eclipse, the predominant ionospheric perturbations were related to irregular EUV illumination caused by two solar active regions [cf. *Mrak* et al., 2018]. Nevertheless, the presence of the background TIDs is apparent, and appears as a modulation, superposed on the eclipse modification. The TIDs were apparent in the same spatial domain as they were prior to the eclipse. Figure 2 shows a snapshot at 18:42 UT, when the totality was already exiting the continental US. The TID wave field is clearly visible as a superposed modulation over the dominant eclipse modification. Figure 2b encompasses merged ΔTEC map and tropospheric weather map, where the red ’X’ mark denotes a region of most intense precipitation (reflectivity >= 60 dBZ), and dashed fiducial circles bolster the apparent concentric figure, with a center in the thunderstorm system.

The wave period was computed for three locations, marked as colored ’X’ marks in Figure 2a, utilizing the time dependent Fourier transform with a fully overlapping 2 hour window, and the Hamming window function. Figure 2c shows example ΔTEC time series for the three locations, and Figure 2d shows a representative spectrogram at the mid-point (90°W, 40°N, red ’X’). The spectrogram shows TID frequency range, with a persistent components clustered in a range from 0.5 – 1 mHz (periods T_p = 16.6 – 33.3 min) between 13 – 20 UT. The peak in the TID waves is centered at ~0.75 mHz, which correspond to a wave period T_p = 22 min. The most prominent wave activity however, is centered at 0.35 mHz (T_p = 55 min) which was caused by the eclipse inducted EUV modulation [*Mrak* et al., 2018].

Figure 3 shows contemporary maps of tropospheric reflectivity as observed by the Next Generation Weather Radar (NEXRAD). Comparing with Figures 1 and 2, there is a notable spatiotemporal correlation between the TIDs and thunderstorm activity. At the beginning (~13 UT), the apparent center of TIDs was near 95°W, 43°N (Iowa), and they were actively generated up until ~14 UT when the causative thunderstorm broke apart. The chronological progress of the TID wave-field is depicted in a longitudinal keogram in Figure 4a. After the initial thunderstorm collapsed, the western edge of TID wave field slowly moved toward east, until a subsequent wavefronts emerged further west at ~15:30 UT (Figure 4a an supplemental video S1), this time with an apparent center close to 100°W, 44°N (South Dakota). The resulting TIDs are seen in $T\Delta EC$ maps and keogram analysis in Figure 4. The TID wave-field resided there up until ~19 UT. A similar pattern is seen in the NEXRAD reflectivity maps (Figure 3 and supplemental video S2): until ~14 UT, there was a strong, almost stationary thunderstorm over Iowa (Figures 3a-b), then the thunderstorm slowly disappeared and a new thunderstorm system strengthened over South Dakota (Figures 3c-d) which lasted then for hours. We indicate a region of biggest reflectivity on each panel with red 'X'. Most storm systems however, had a reflectivity value >20 dBZ, which can be in general enough to produce deep convective plumes [*Vadas et al.*, 2012]. We direct the reader to watch supplemental videos S1 and S2, showing ionospheric and tropospheric weather evolution, respectively.

We examine the TEC perturbations in greater details here. Figure 4 consists of two keograms oriented along longitude and latitude (a,b), for the day of the eclipse. The TIDs emerged at ~13 UT with a longitudinal extent between 100°W and 70W (edge of the GNSS coverage), the line of emanation is well aligned with a 90 minutes delayed local sunrise time (Figure 4a). The longitudinal keogram elongated along 40°N latitude shows a fairly constant slope (zonal velocity (v_x)) of the TIDs as a function of longitude and time. The only notable modification was at ~16 UT, when the slope slightly increased. The zonal velocity v_x at 40°N latitude changed from ~140 m/s to ~180 m/s; the time of the change is aligned with the new front of TIDs with a center of the second thunderstorm system. The latitudinal keogram 4b shows the TIDs over the same time period with a bent wavefronts. The wavefronts are vertical at ~43°N (13–14 UT), and the slope northward and southward is bent in opposite propagation directions. The wavefronts' shape implies the source/center was located near ~43°N at that time. The mean meridional velocity v_y of the TIDs, extracted from keogram 4b is ~170 m/s before, and ~140 m/s after the change. Therefore, the horizontal propagation velocity v_h of the TIDs is estimated to be ~220 m/s, propagating radially away from the source. The change of velocity components over time resulted in a minor change in the speed: from 220 m/s at the beginning to 230 m/s after the modification. The observed change in velocity components suggests its source had moved. In addition, we show a closer look at the TIDs during the eclipse time period in Figure 4c. It is nicely seen, that the large scale perturbations were modulated with a secondary wave field. While the modulation effect is barely seen near the region of maximum obscuration (~100°W), the modulation is becoming evident in the direction eastward toward regions of smaller eclipse effect. The modulation is, however, co-linear with the TIDs existing before the arrival of the eclipse.

We performed a 2D Fourier analysis of keograms 4a and 4b, to determine the dominant wave numbers of the TEC perturbations for the day of the eclipse. The spectrograms in Figure 5 show persistent waves, with wave numbers clustered in ranges k_x = [0.025,0.08] km^{-1} in the zonal direction, and k_x = [0.015,0.04] km^{-1} in the meridional direction. The corresponding wavelength components are λ_y = [160, 420] km and λ_x = [80, 250] km. A mean horizontal wavelength λ_h is ~350 km. However, it is impossible to retrieve the horizontal wavelength components of concentric waves in a non-radial direction. Therefore, we name ranges of existing wavelength components along single meridional and zonal lines, retrieved from spectrograms in Figure 5. The center of the concentric TIDs was not stationary, therefore a keogram analysis in the thunderstorm frame of reference would we convoluted.

In addition, ionospheric electron density perturbations on the eclipse day was strikingly similar to the day before (20 August 2017). An illustrative example is depicted in Figure 6, where ΔTID map has overlaid radar reflectivity map. Fiducial circles indicate concentric nature of the observed TIDs, again having a center in the storm system. The TIDs on that day resided over nearly the same region in space, while the timing of the TIDs' appearance was also nearly synchronized. The TIDs emerged from the background ionosphere at ~13 UT, which is about 1.5 hours after local sunrise (sunrise was at ~11:30 UT, at 90°W, 40°N). The TIDs also emerged everywhere at the same time, implying that the source of the TEC perturbations was present earlier, but their imprint in the ionosphere was revealed only after ionospheric production initiated. Supplementary videos S3 and S4 show TID and thunderstorm activity on that day, respectively.

The obtained wave parameters are in agreement with previous studies of thunderstorm/weather induced GWs [e.g. *Azeem et al.*, 2015; *Azeem and Barlage*, 2017; *Chou et al.*, 2017]. Furthermore, the estimated vertical wavelength λ_z for no background wind, taking the mean apparent horizontal wavelength λ_h=350 km, and buoyancy period T_b=10.5 min, at 250 km altitude from the NRLMSISE-00 model is:

$$\lambda_z = \sqrt{\frac{T_b^2}{T_p^2 - T_b^2} \cdot \lambda_h^2} = 190 \text{ km}, \quad (1)$$

which is enough to cause a prominent compression/ratification of the ionosphere in the vicinity of the F-peak, as previously identified by *Azeem and Barlage* [2017]. The horizontal angle Θ of GWs propagation was

$$\Theta = \arctan \frac{\lambda_z}{\lambda_h} = 28.5^{\circ}. \quad (2)$$

Utilizing a simplified expression [*Vadas et al.*, 2012] for vertical group velocity, c_{gz}, we obtain:

$$c_{gz} \approx \frac{\lambda_h^2 T_b^2}{\lambda_z T_p^3} = 111 \text{ m/s}. \quad (3)$$

The propagation time for these GWs to reach 250 km altitude is thus ~36 min, which implies there is a non-negligible time lag between tropospheric and ionospheric weather. It should be noted that a propagation time is usually longer (40–90 min), utilizing a gravity wave dispersion relation [*Yue et al.*, 2009].

4 Discussion

We present extended observations of ionospheric perturbations on the day of the total solar eclipse. We show concentric/elliptical TIDs, which resided over central US, they propagated in east/southeast direction and had an apparent center in a causative thunderstorm system. The TIDs resided in the same position in space for a time period of ~6 hours. The TIDs had a zonal wavelength range λ_x=[80, 250] km, meridional wavelength range λ_y=[160, 420] km, with a dominant horizontal wavelength $\lambda_h \approx$350 km. The propagation speed was ~220 m/s radially away from the source, predominantly in east/southeast direction. Further, estimated TID wave period range of the TIDs at 90°W, 40°N, T_p = [16.6, 23.8] min, with an estimated mean value of $T_p \approx$22 min.

Estimated TID parameters are well withing the range of previously reported tropospheric weather initiated GWs and/or subsequent TIDs [e.g., *Vadas and Nicolls*, 2008; *Yue et al.*, 2009; *Vadas et al.*, 2012; *Lay* et al., 2013; *Azeem et al.*, 2015; *Azeem and Barlage*, 2017; *Chou et al.*, 2017], as well as the ones reported by *Zhang et al.* [2017]. The eclipse, however, did appear to alter the dominant wavelength and speed of the TIDs. This observation is a straightforward consequence of eclipse induced erosion of the E-region. The peak momentum flux carried by a GW is at an altitude between 150-200 km at solar minimum [*Vadas and Fritts*, 2006]. Therefore the erosion of the bottom side ionosphere raised the GW-TID coupling altitude to a region of higher temperature. The resulting TIDs within the eclipse should thus appear with larger horizontal phase speed and increased wavelengths [*Vadas and Fritts*, 2006; *Vadas*, 2007]. Namely, the eclipse affected the TID wave field, however the effect was the one of modulation rather than the one of production.

Another eclipse modification can be seen as a temporary disappearance of the TIDs in the leading half of the penumbra. *Yue et al.* [2009] did a climatological study of concentric GWs, caused by tropospheric weather, and found that they occur only at times of the weakest neutral wind (May-June and August-September, with winds weaker than 20 m/s) in the mesosphere/stratosphere. Additionally, *Harding et al.* [2018] showed a huge wind modification carried by the penumbra, with the wind direction pointing toward the totality, and with winds exceeding 50 m/s right in front of the total obscuration. Therefore, the eclipse imposed winds in that area damped the GWs, since the imposed modification is at least a factor 2 bigger than the background winds, hence no TIDs were observed there.

Considering the extended set of observations, including ionospheric TIDs and the weather activity fully covered in supplemental movies S1 – S4, we argue that the TIDs trailing the totality were not initiated by the eclipse. Instead, they resemble the same source field as prior to the eclipse. If the waves would have been triggered by the eclipse, then the TIDs should be apparent along its entire path. Instead, the waves were spatially confined only to the region of the prior TID wave-field. The apparent concentric/elliptical shape and the source region indeed coincides with the path of the totality, which can be a deceiving factor. Nonetheless, the actual center of the TIDs was slightly northward from the totality track (~3° lat), which breaks the symmetry that would be expected if the source was the eclipse. Further, the center of the TIDs (Figure 2) spatially matched the center of the thunderstorm over South Dakota (Figure 3c-d).

Another observation that deserves discussion is the timing of the waves apparent behind the totality region. As we calculated in Eq.(3), the apparent waves propagate vertically with a speed ~110 m/s. If the source would be the stratospheric cooling [*Chimonas and Hines*, 1970], then it would take $\Delta t = \Delta z / c_{gz}$ ≈ 33 min to reach 250 km altitude. However, the TIDs trailing the totality became apparent ~10 min behind the totality. Namely, close to a region where the neutral winds abate, and change the direction [cf. *Harding et al.*, 2018]. If the source of the TIDs were the eclipse, the source altitude would reside at $\Delta z = \Delta t\, c_{gz}$ ≈ 66 km; at an altitude of 184 km (250 km – 66 km).

The "bow waves" interpretation is also problematic on theoretical grounds. Both *Liu* et al. [2011] and *Zhang et al.* [2017] linked their observations to the original prediction by *Chimonas and Hines* [1970], and subsequent steady state analysis [*Chimonas*, 1970]. But at ionospheric heights, the bow waves anticipated by *Chimonas* [1970] should have a wavelength of ~1000 km, and reside at a lateral distance of ~10,000 km away from the totality track. A more thorough calculations by *Fritts and Luo* [1993] further confirmed these parameters, with results in the same magnitude range as obtained by *Chimonas* [1970]. Even a more recent treatment of the same problem, invoking a comprehensive first principles analysis [*Eckermann et al.*, 2007], confirmed these predictions. In summary, the physics based modeling efforts do predict bow waves of the stratospheric origin at ionospheric heights. However, the waves should have the following parameters: (i) Horizontal wavelength ~1000 km, (ii) lateral extent of ~10,000 km, and (iii) the waves should lag the totality by ~1 hour [*Eckermann et al.*, 2007]. The observed TIDs, also claimed as the "bow waves" [*Zhang et al.*, 2017] are in stark disagreement with theoretical predictions, adding further support for the alternate source mechanism we have identified.

Curiously, there are recent studies that confirmed the existence of the eclipse generated bow wave in the thermosphere for this eclipse. Namely, *Harding et al.* [2018] showed the observational evidences for thermospheric bow wave, while *Lin* et al. [2018] and *Lei* et al. [2018] showed a modeled thermospheric/ionospheric bow wave. However, it should be noted that the latter authors observed an evanescent *in situ* generated bow wave [*Ridley et al.*, 1984], and not a wave field generated at stratospheric heights.

5 Summary

The geospace is extremely complicated and entangled system which demands a careful examination, even if perturbed by a controlled experiment. We demonstrated the complexity of systematic deconvolution of integrated and simultaneous driving of the Earth's ionosphere. The eclipse provided a marvelous sign of a "pinhole" projection of solar active regions, and a simultaneous projection of tropospheric weather as we demonstrated here. In this letter, we discussed the most likely origin of the accompanying traveling concentric ionospheric disturbances by virtue of concurrent observations of tropospheric and ionospheric weather. We found the presence of TID waves that emerged 5 hours before the arrival of the eclipse, and which persisted throughout the penumbra. We find that:

1. The apparent centers of the TIDs coincided with locations of tropospheric thunderstorms.
2. TID wave analysis revealed consistency with previously described tropospheric weather-initiated GWs and subsequent TIDs.
3. The coincidental appearance of the TIDs can be explained by means of the eclipse timing, which happened in the month of August: a month of weakest neutral winds that allow GWs to propagate into thermosphere/ionosphere.
4. Based upon a consideration of other observations and modeling results, we ruled out the eclipse source as a possible physical source of the observed concentric TIDs.

In summary, we have observed a myriad of unexpected and intriguing ionospheric phenomena during the August 2017 total solar eclipse, owing to the best remote sensor coverage in the history of eclipse observations. We report extensive TID activity on that day, which was most likely the ionospheric manifestation of thunderstorm-initiated GWs, and not produced by the eclipse. The findings are important because there is an extensive eclipse modeling effort ongoing for this event as well as forthcoming total solar eclipses. We argue that without consideration of the tropospheric convective storms at the locations identified herein, one will not be able to reproduce the observed TIDs.

Acknowledgments

This work was supported by the National Science Foundation under grant AGS-1743832. The TEC maps were created using data from the CORS database publicly available on ftp://geodesy.noaa.gov/cors/, and CDDIS database ftp://ftp.cddis.eosdis.nasa.gov/gps/data/daily/. Totality track was obtained from https://eclipse.gsfc.nasa.gov/SEpath/SEpath2001/SE2017Aug21Tpath.html. NEXRAD radar data was acquired through [*Hirsch*, 2018], using publicly available database: https://mesonet.agron.iastate.edu/archive/data/

References

Azeem, I., J. Yue, L. Hoffmann, S. D. Miller, W. C. Straka III, & G. Crowley (2015), Multi-sensor profiling of a concentric gravity wave event propagating from the troposphere to the ionosphere, *Geophys. Res. Lett.*, 42,7874-7880, doi:10.1002/2015GL065903.

Azeem, I., J. & M. Barlage, (2017), Atmosphere-ionosphere coupling from convectively generated gravity waves, *Advances in Space Research*, 61, 1931-1941, doi:10.1016/j.asr.2017.09.029.

Chou, M. Y., C. C. H. Lin, J. Yue, H. F. Tsai, Y. Y. Sun, J. Y. Liu, and C. H. Chen (2017), Concentric traveling ionosphere disturbances triggered by Super Typhoon Meranti (2016), Geophys. Res. Lett., 44, 1219-1226, doi:10.1002/2016GL072205.

Chimonas, G., and C. O. Hines (1970), Atmospheric gravity waves induced by a solar eclipse, *J. Geophys. Res., space Physics*, 75, 875, doi:10.1029/JA075i004p00875.

Chimonas, G. (1970), Internal Gravity - Wave Motions Induced in the Earth's Atmosphere by a Solar Eclipse, *J. Geophys. Res., space Physics*, 51, 28, 5545-5551, doi:10.1029/JA075i028p05545.

Coster, A., J., Gaposchkin, E., M., and Thornton, L., E., (1992), Real-Time Ionospheric Monitoring System Using GPS, *Journal of The Institute of Navigation*, 38, 2, doi:10.1002/j.2161-4296.1992.tb01874.x.

Coster, A., D. Herne, P. Erickson, and D. Oberoi (2012), Using the Murchison Widefield Array to observe midlatitude space weather, *Radio Sci.*, 47, RS0K07, doi:10.1029/2012RS004993.

Coster, A. J., Goncharenko, L., Zhang, S.-R., Erickson, P. J., Rideout, W., & Vierinen, J. (2017). GNSS Observations of ionospheric variations during the 21 August 2017 solar eclipse. *Geophysical Research Letters*, 44. https://doi.org/10.1002/2017GL075774.

Eckermann, S. D., D. Broutman, M. T. Stollberg, J. Ma, J. P. McCormack, and T. F. Hogan (2007), Atmospheric effects of the total solar eclipse of 4 December 2002 simulated with a high-altitude global model, *J. Geophys. Res.*, 112, D14105, doi:10.1029/2006JD007880.

Fritts, D. C., and Z. Luo (1993), Gravity wave forcing in the middle atmosphere due to reduced ozone heating during a solar eclipse, *J. Geophys. Res.*, 98(D2), 3011-3021, doi: 10.1029/92JD02391.

Grawe, M. A., and J. J. Makela (2015), The ionospheric responses to the 2011 Tohoku, 2012 Haida Gwaii, and 2010 Chile tsunamis: Effects of tsunami orientation and observation geometry, *Earth and Space Science*, 2, 472-483, doi:10.1002/2015EA000132.

Harding, B. J., Drob, D. P., Buriti, R. A., & Makela, J. J. (2018). Nightside detection of a large-scale thermospheric wave generated by a solar eclipse. Geophysical Research Letters, 45, 3366-3373. doi:10.1002/2018GL077015.

Hirsch, Michael (2018), NEXRADutils (Software), doi 10.5281/zenodo.1402629.

Klobuchar, J. A., (1987), Ionospheric Time-Delay Algorithm for Single-Frequency GPS Users, *IEEE Transactions on Aerospace and Electronics Systems*, 23-2, doi: 10.1109/TAES.1987.310829.

Lay, E. H., X.-M. Shao, and C. S. Carrano (2013), Variation in total electron content above large thunderstorms, *Geophys. Res. Lett.*, 40, 1945âĂŞ1949, doi:10.1002/grl.50499.

Lei, J., Dang, T., Wang, W., Burns, A., Zhang, B., & Le, H. (2018). Long-lasting response of the global thermosphere and ionosphere to the 21 August 2017 solar eclipse. *Journal of Geophysical Research: Space Physics*, 123, 4309âĂŞ4316 doi:10.1029/2018JA025460.

Lin, C. Y., Y. Deng, and, A. Ridley, (2018), Atmospheric Gravity Waves in the Ionosphere and Thermosphere During the 2017 Solar Eclipse, *Geophys. Res. Lett.*, in press, doi:10.1029/2018GL077388.

Liu, J.Y., Sun, Y.Y., Kakinami, Y., Chen, C.H., Lin, C.H., Tsai, H.F., Bow and stern waves triggered by the Moon's shadow boat: SOLAR ECLIPSE BOW AND STERN WAVES (2011). *Geophys. Res. Lett.* 38, doi:10.1029/2011GL048805.

Mrak, S., J. Semeter, D. Drob, and J.D. Huba, (2018), Direct EUV/X-ray Modulation of the Ionosphere during the August 2017 Total Solar Eclipse, *Geophys. Res. Lett.*, in press, doi:10.1029/2017GL076771.

Nishioka, M., T. Tsugawa, M. Kubota, and M. Ishii (2013), Concentric waves and short-period oscillations observed in the ionosphere after the 2013 Moore EF5 tornado, *Geophys. Res. Lett.*, 40, 5581-5586, doi:10.1002/2013GL057963.

Nykiel, G., Y. M. Zanimonskiy, Y. M. Yampolski, and M. Figurski, (2017), Efficient Usage of Dense GNSS Networks in Central Europe for the Visualization and Investigation of Ionospheric TEC Variations *Sensors*, 17, 2298, doi:10.3390/s17102298.

Ridley, E. C., R. E. Dickinson, M. H. Rees, and R. G. Roble, (1984), Thermospheric Response to the June 11, 1983, Solar Eclipse, *J. Geophys. Res.*,89,A9, PAGES 7583-7588,

Tsugawa, T., Y. Otsuka, A. J. Coster, and A. Saito (2007), Medium-scale traveling ionospheric disturbances detected with dense and wide TEC maps over North America, *Geophys. Res. Lett.*, 34, L22101, doi:10.1029/2007GL031663.

Tsugawa, T., Saito, A., Otsuka, Y. et al. (2011), Ionospheric disturbances detected by GPS total electron content observation after the 2011 off the Pacific coast of Tohoku Earthquake, *Earth Planet Sp*, 63:66. doi:10.5047/eps.2011.06.035.

Vadas, S. L., and D. C. Fritts (2006), Influence of solar variability on gravity wave structure and dissipation in the thermosphere from tropospheric convection, *J. Geophys. Res.*, 111, A10S12, doi:10.1029/2005JA011510.

Vadas, S. L. (2007), Horizontal and vertical propagation and dissipation of gravity waves in the thermosphere from lower atmospheric and thermospheric sources, *J. Geophys. Res.*, 112, A06305, doi:10.1029/2006JA011845.

Vadas, S. L., and M. J. Nicolls (2008), Using PFISR measurements and gravity wave dissipative theory to determine the neutral, background thermospheric winds, *Geophys. Res. Lett.*, 35, L02105, doi:10.1029/2007GL031522.

Vadas, S., J. Yue, and T. Nakamura (2012), Mesospheric concentric gravity waves generated by multiple convective storms over the North American Great Plain: CONCENTRIC GRAVITY WAVES, *J. Geophys. Res.*, 117, D07113, doi:10.1029/2011JD017025.

Yue, J., S. L. Vadas, C.-Y. She, T. Nakamura, S. C. Reising, H.-L. Liu, P. Stamus, D. A. Krueger, W. Lyons, and T. Li (2009), Concentric gravity waves in the mesosphere generated by deep convective plumes in the lower atmosphere near Fort Collins, Colorado, *J. Geophys. Res.*, 114, D06104, doi:10.1029/2008JD011244.

Zhang, S.-R., Erickson, P. J., Goncharenko, L. P., Coster, A. J., Rideout, W., and Vierinen, J. (2017). Ionospheric bow waves and perturbations induced by the 21 August 2017 solar eclipse. *Geophys. Res. Lett.*, 44, doi:10.1002/2017GL076054.

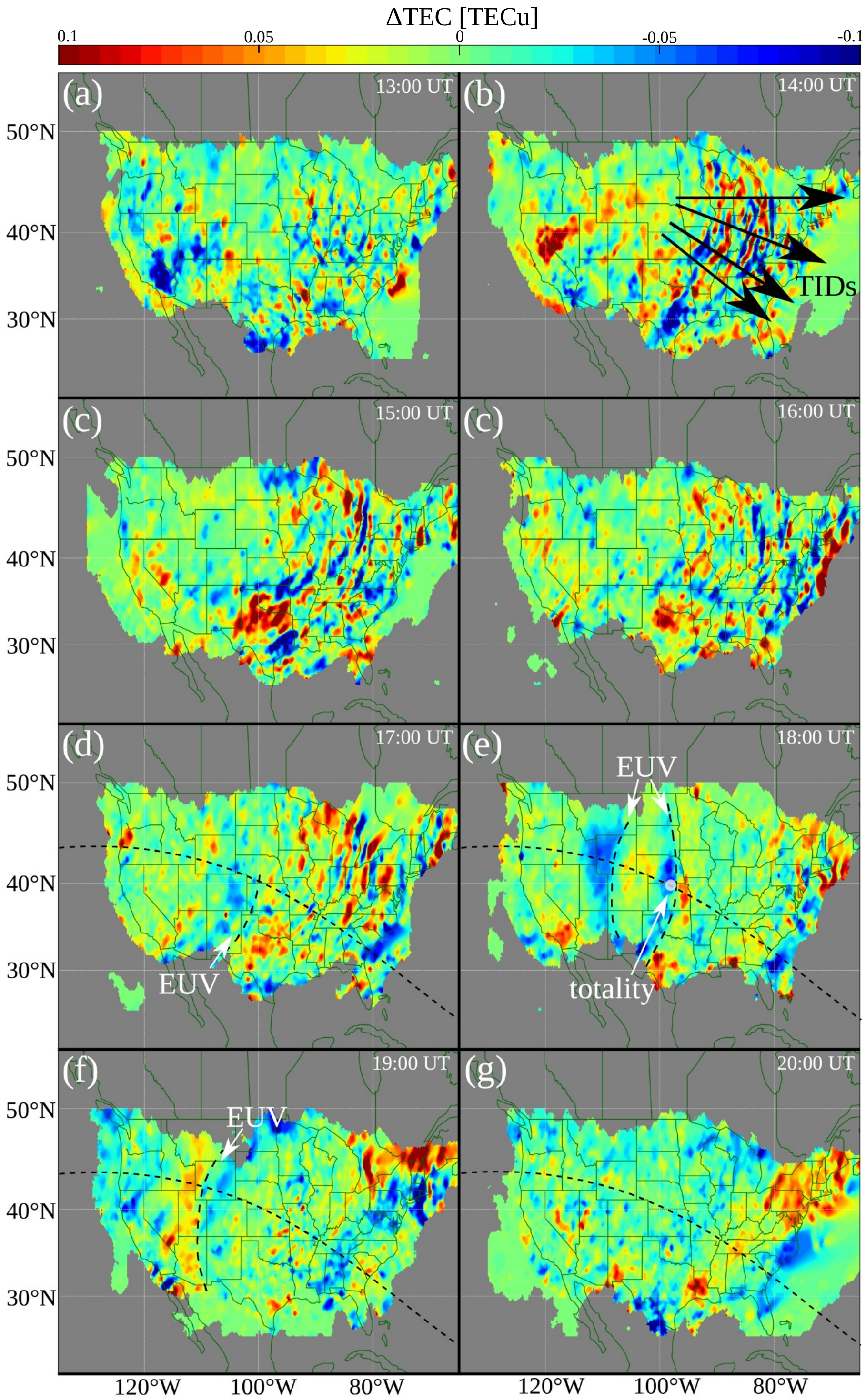

Figure 1. (a)-(g) 21-August, 2017: Differential TEC ΔTEC images, mapped at 300 km altitude, showing extensive TID activity over central and eastern US. The arrows in (b) indicate propagation direction of underlying TIDs. The black fiducial dashed line in (d)-(f) indicates the path of totality. (d)-(f) Dashed lines indicate positions of large scale TEC perturbations due to uneven EUV flux. (e) White circle indicates the position of the total eclipse at the given time.

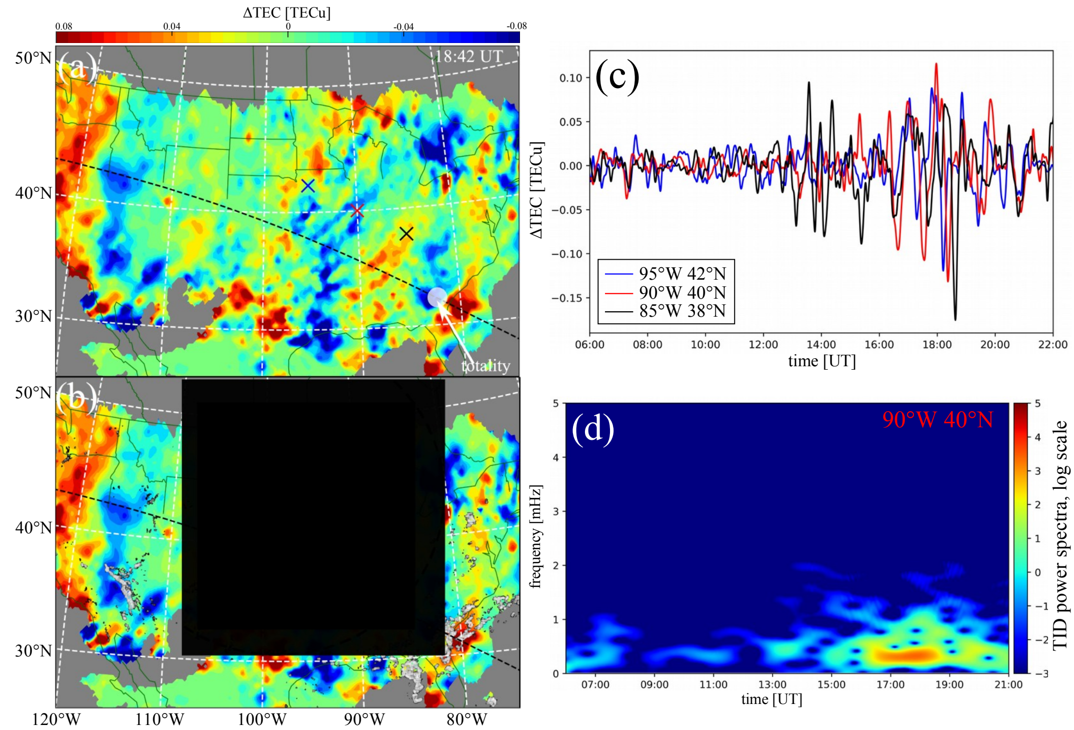

Figure 2. (a) An image of traveling ionospheric disturbances trailing the totality (white circle), the TIDs are modulated on top of the salient eclipse inducted modification. The image bolster simultaneous and co-operative forcing of the ionosphere from below (TIDs) and from above (large scale TEC perturbations). (b) Same as panel (a), with an overlay of tropospheric weather storms (gray) from the NEXRAD maps. Red 'X' denotes a position of the most intense precipitation inside the storm system. Dashed fiducial lines emphasize concentric nature of the TIDs, with a center in the storm system, center if the red 'X'. (c) Time series plot of ΔTEC perturbations for three regions identified 'X' in panel (a). (d) A representative spectrogram of ΔTEC at 90°W, 40°N.

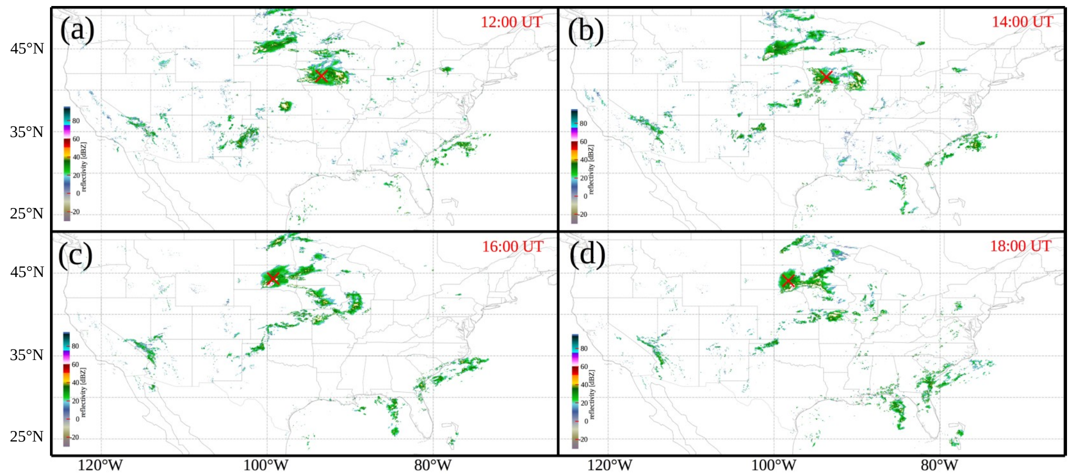

Figure 3. (a–d) NEXRAD radar reflectivity maps of thunderstorm activity for the day of the eclipse. Each image show an identified center (red cross 'X') of the most intense thunderstorm. The NEXRAD maps were produced by NEXRAD-quick-plot software [*Hirsch*, 2018]

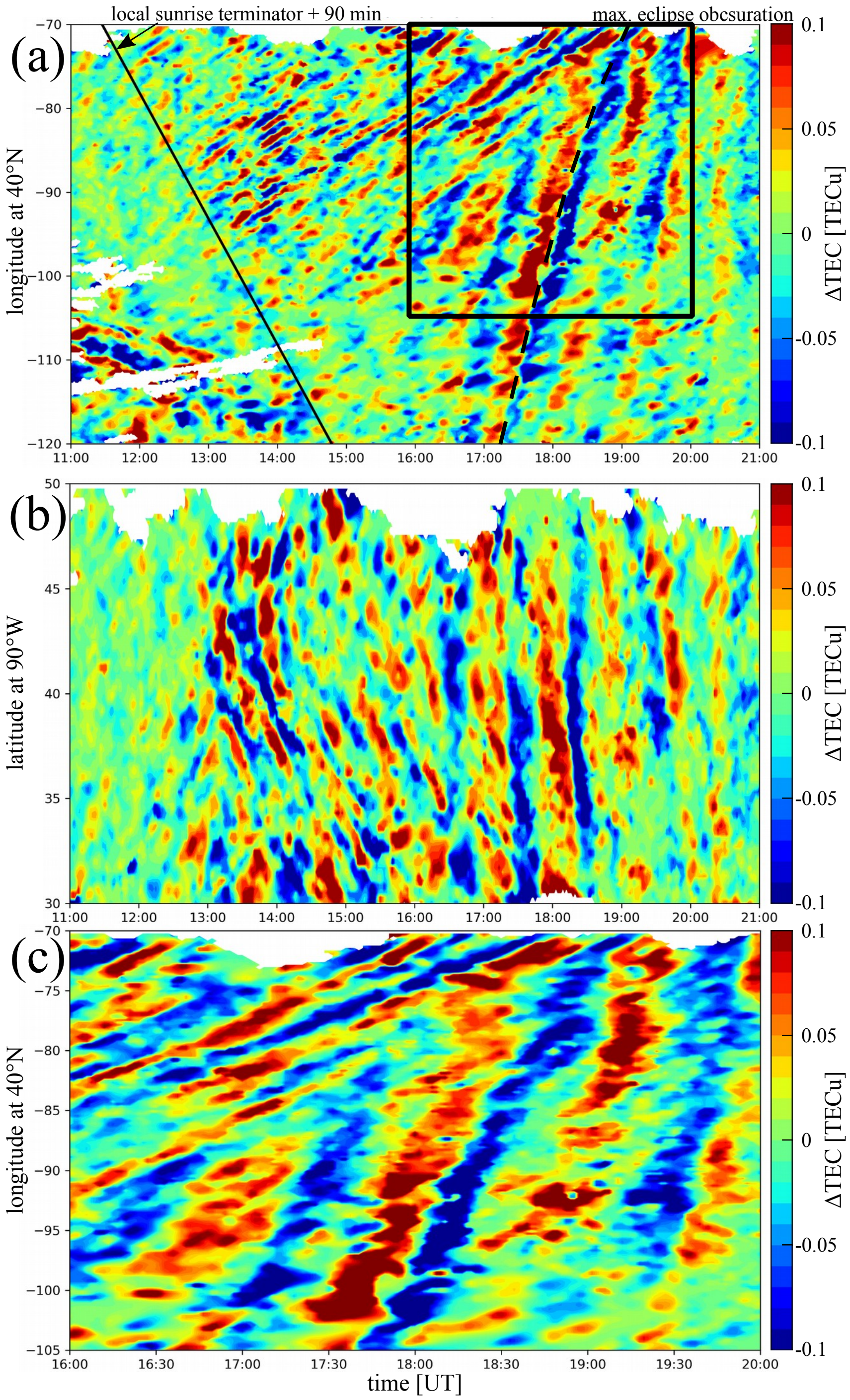

Figure 4. A set of TID keograms on the day of the eclipse. (a-b) longitudinal cut at 40°N and latitudinal cut at 90°W, respectively. (a) Solid black fiducial line is a local sunrise terminator delayed for 90 minutes; dashed fiducial line is a line of the biggest obscuration at the chosen latitude; black box is a region shown in panel (c).

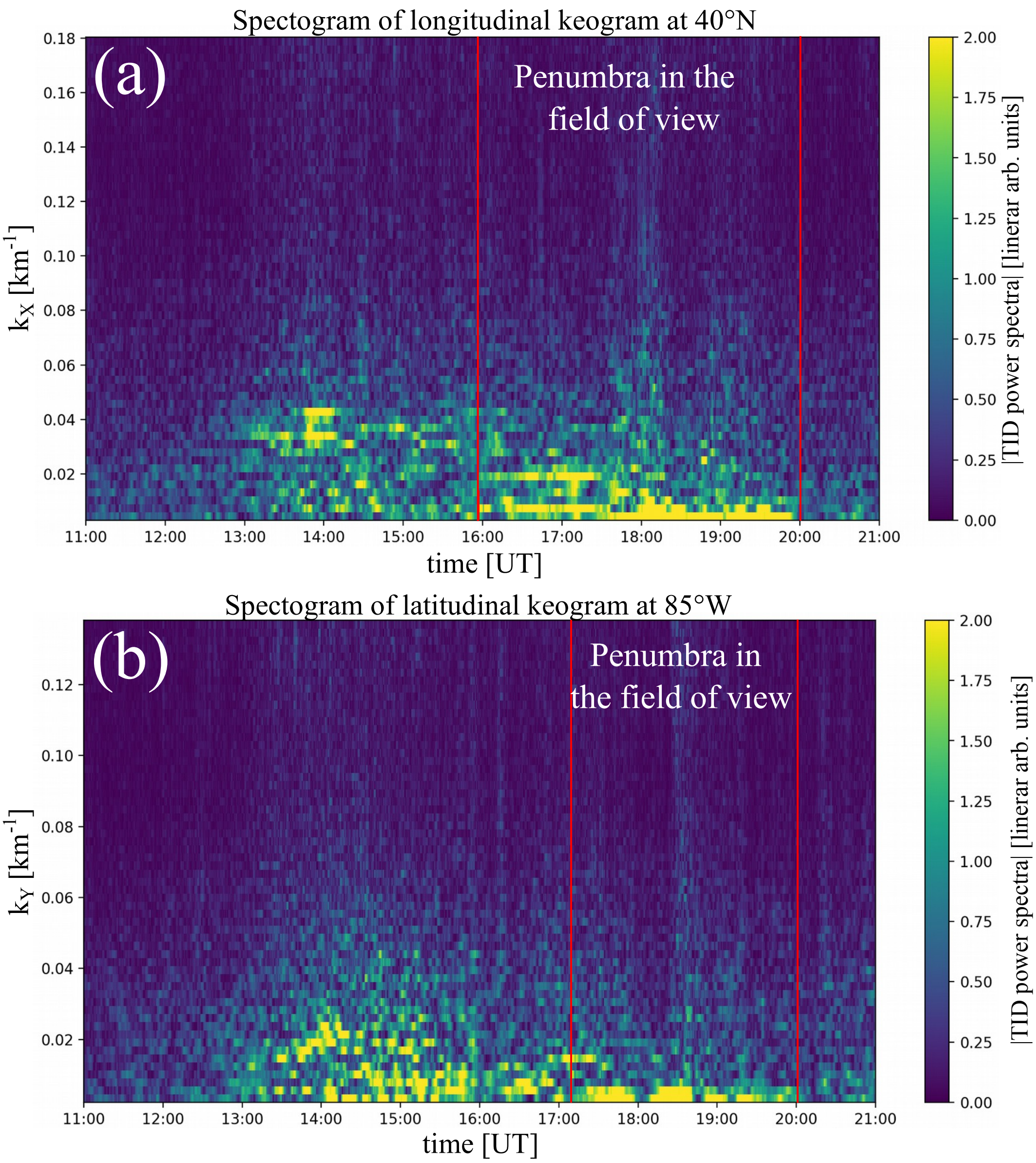

Figure 5. Spectrograms of the keograms 4a and 5b, respectively. (a) Wave number decomposition in the zonal direction (k_x). (b) Wave number decomposition in the meridional direction (k_y). The red fiducial lines indicate a time range of the eclipse present in a field of view. Intensity of the spectrogram is TID power spectra in linear scale.

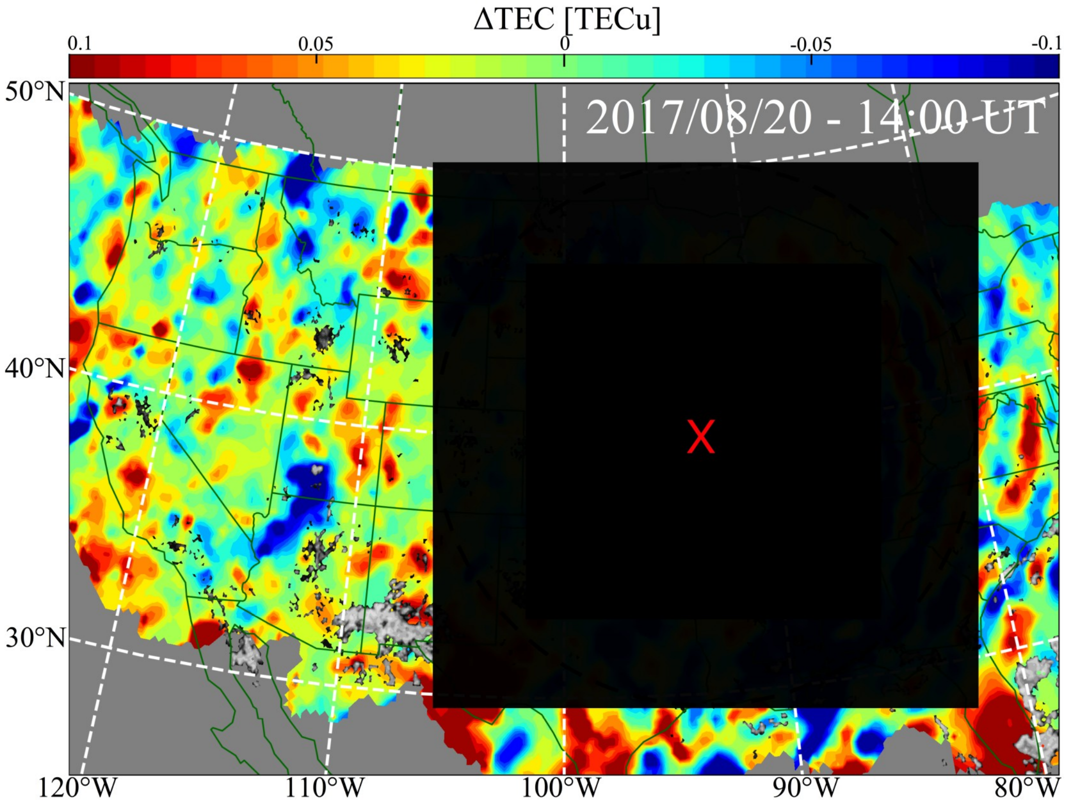

Figure 6. A snapshot of contemporary images of ionospheric (ΔTEC) and tropospheric (NEXRAD) weather maps on 20 August, 2017 (the day prior to the eclipse). The map is a snapshot taken at 14:00 UT, ΔTEC map (color-coded) is projected to 300 km altitude, NEXRAD maps is Gray-shaded. Red mark 'X' is a region of biggest reflectivity (check supplemental video S4), and dashed circles match the TID pattern, and have center in red 'X'.